Origin of enhanced cold crystallization rate for freeze-dried poly(L-lactide) from solutions

Origin of Enhanced Cold Crystallization Rate for Freeze-dried Poly(L-lactide) from Solutions

Takashi Sasaki, Daisuke Morino, Nobuaki Tabata

Department of Materials Science & Engineering, University of Fukui, Bunkyo, Fukui 910 8507, Japan.

Correspondence to: Takashi Sasaki; e-mail: sasaki@matse.u-fukui.ac.jp

Abstract

Poly(L-lactide) (PLLA) freeze-dried from dilute 1,4-dioxane solutions exhibited very porous structure composed of thin membranes of which the mean thickness was estimated to be 104 – 135 nm. Heating measurements of differential scanning calorimetry (DSC) showed that the freeze-dried PLLA (FDPLLA) exhibits an exothermic peak due to cold crystallization at 78 – 81°C, which is at least 20 K lower than that for a quenched amorphous bulk PLLA. In accord with this, the overall rate of isothermal cold crystallization was revealed to be greater for the FDPLLA than that for the bulk. The origin of such high crystallizability of FDPLLA is attributed to its large surface area where the chain mobility is greater than in the bulk PLLA. The exothermic peak in the DSC trace shifted to a further lower temperature when the FDPLLA is immersed in ligroin (non-solvent), which also suggests a major role of the free surface in enhancing the cold crystallization rate. On the other hand, the density and the chain conformational feature of the FDPLLA were revealed to be identical to the bulk PLLA.

INTRODUCTION

Freeze-drying a polymer solution is expected to yield a very small-sized geometry as finely divided powder or porous material of the polymer. The effects of freeze-drying from a dilute solution on the glass transition temperature (T_g) and on the cold crystallization behaviors have been investigated so far, and the mechanism for these effects have been attributed to the specific feature of freeze-dried state such as less interpenetrated structures [1-9]. However, results that contradict the existence of the specific structure in freeze-dried polymers have also been reported [10,11]. In addition, it has been demonstrated that the T_g depression, which was frequently reported for freeze-dried polymers, is simply due to residual solvent [12]. Thus, experiments have to be done very carefully in order to investigate the thermal behaviors of freeze-dried polymers.

In a previous paper, we have shown that for poly(L-lactide) (PLLA) freeze-dried from very dilute 1,4-dioxane solutions (0.07 – 0.52wt%), the T_g is lowered from that of a bulk amorphous sample, and that an exothermic peak due to cold crystallization observed during heating scan of differential scanning calorimetry (DSC) appears at a temperature 20 – 30 K lower than that for the bulk amorphous PLLA [9]. Our supplementary experiments have revealed that the T_g depression is mainly originated from the residual solvent for the PLLA/1,4-dioxane system, which is consistent with the results for freeze-dried polystyrene [12]. However, even for the freeze-dried PLLAs that were prepared carefully by removing the residual solvent with additional vacuum drying process, we have still observed depression of the cold crystallization temperature T_c; here we define T_c as the peak temperature of the exotherm due to cold crystallization in DSC heating trace. This suggests that certain structural features intrinsic to the freeze-dried PLLA (FDPLLA) exist. Furthermore, in contrast to the T_g behavior, the T_c depression has been observed even for the samples from highly concentrated solutions of up to 7.0wt%, which is well above the critical concentration of chain overlapping. This indicates that the idea of less overlapping in not the origin of the T_c depression. In this study, we elucidate further the cold crystallization behaviors of FDPLLA comparing with a bulk amorphous PLLA, perform structural characterizations by means of wide-angle X-ray scattering (WAXS), Fourier transform infrared (FT-IR) spectroscopy, and density and specific surface area measurements, and try to understand

the origin of the high crystallizability characteristic to the FDPLLA.

EXPERIMENTAL

PLLA used in this study was supplied from Mitsui Chemicals Co.; M_w = 210 kg mol^{-1} with 98% L units. 1,4-Dioxane was purchased from Nacalai Tesque Inc., and was distilled before use. Ligroin (boiling range: 90 – 125°C) and bromobenzene were used as-received from Wako Pure Chemical Industries and Nacalai Tesque Inc., respectively. PLLA was first heated at 190°C for 3 min and pressed at 100 kg cm^{-3} for 5 min followed by rapid quenching in a water bath (ca. 20°C) to make completely amorphous PLLA sheets of 0.1 – 0.5 mm thick. The obtained PLLA sheets were added to 1,4-dioxane, and completely homogeneous solutions with different concentrations (C_0 = 0.09, 0.50, and 5.0wt% PLLA content) were prepared by stirring the mixture for 168 h at room temperature. The solution was frozen very rapidly by pouring it drop by drop directly into liquid nitrogen. The frozen material was then dried under vacuum for 30 h by using a vacuum line apparatus (10^{-5} Torr). The ambient temperature was not controlled (20 – 25°C). The reduced pressure achieved by the vacuum line was obviously below the triple point of the solvent so that melting was not observed during the sublimation process [9].

Sphere-shaped freeze-dried particles (1 – 2 mm in diameter) with high porosity were yielded as typically shown in Fig. 1. The obtained particles are originated from solution droplets in the rapid freezing process. The as-freeze-dried samples were further dried under vacuum at 40°C for 168 h to remove completely the residual solvent. We confirmed that no weight loss (less than 0.01%) is detected even after annealing the sample at 185°C for 3 min, while weight loss of 0.4 – 0.6wt% was detected when the above additional vacuum drying was not applied. To prevent hydrolysis as well as any structural relaxation, the obtained FDPLLA was stored at –27°C until any further measurements were taken. As a reference bulk amorphous PLLA, we used the amorphous sheets prepared above. These bulk specimens were further subject to the same treatment of vacuum drying as above (annealed at 40°C for 168 h) in order to conform the thermal history to that of the FDPLLA.

DSC measurements were performed by using a calorimeter Perkin Elmer Pyris Diamond equipped with a cooling system Perkin Elmer Intra-cooler P2 that was

operated at –88°C. All measurements were done under nitrogen atmosphere. The temperature and heat flow were calibrated using an indium standard. We used usual aluminum pans Perkin Elmer 0219-0041 for the solid samples, and large volume stainless steel capsules Perkin Elmer 0319-0218 for the samples of PLLA/ligroin mixture. Prior to the latter measurements, PLLA (both freeze-dried and bulk) was immersed in ligroin for at least 72 h at room temperature so that ligroin permeated completely into the porous PLLA. Step-scan DSC measurements were performed, which gave traces of reversing heat capacity and non-reversing heat flow. In the step-scan mode, we repeated a 2 K step of heating that was achieved with a rate of 5 K min^{-1}, followed by a temperature holding segment of 1.5 min. To check the reproducibility of the results, multiple measurements were performed for ten different specimens. Isothermal cold crystallization rate was measured on the DSC apparatus by detecting exotherm due to cold crystallization after temperature jump (200 K min^{-1}) from 40°C to various crystallization temperatures ranging from 70 to 140°C. The overall crystallization rate G was estimated by a reciprocal of the half-time for reaching the final value of crystallinity, i.e., $G = 1/t_{0.5}$ [13].

WAXS in transmission mode was performed by using an X-ray diffractometer Rigaku R-Axis equipped with a Mo$K\alpha$ radiation source (λ = 0.071 nm) and with a two-dimensional imaging plate as a detector. The collected scattering intensity (I) data were integrated over whole range of azimuthal direction to obtain I vs s ($s = 4\pi \sin\theta / \lambda$) curves. Reliable scattering intensity data were obtained for s = 4 – 85 nm^{-1}. The measurements were done at room temperature.

FT-IR spectroscopy was performed by using a Nicolet Nexus 870 infrared Raman spectrometer (attenuated total reflection measurement). Scanning electron microscopy (SEM) was performed by using a Hitachi S-2600. Specific surface area was determined by the Brunauer-Emmett-Teller (BET) absorption method: adsorption of krypton at 77 K gave a BET adsorption isotherm, from which we determined specific surface area of the FDPLLA. Density difference between the freeze-dried and bulk PLLA samples were investigated by sink-float method: ligroin/bromobenzene mixtures were used and the measurements were taken in a water bath that was controlled at 25.0°C. As the freeze-dried particles are very porous, they were first immersed in ligroin and degassed under vacuum by several pump-thaw cycles until the particles sank

completely to the bottom of glass tube. Bromobenzene was added step by step to this mixture, and equilibration time of more than 10 min was needed for each step.

RESULTS AND DISCUSSION

Cold crystallization behavior

As we have demonstrated previously [9], FDPLLAs from dilute 1,4-dioxane solutions exhibit an exotherm due to cold crystallization at 70 – 80°C during DSC heating of step-scan mode, while an amorphous bulk PLLA exhibits higher exotherm at 100 – 130°C. The present solvent-free FDPLLAs exhibit the same trend of cold crystallization behavior as typically shown in Fig. 2 for the FDPLLA from the solution of C_0 = 5.0wt%: exothermic cold crystallization peak (T_c) is observed at 81°C in the non-reversing heat flow, while for the bulk PLLA, the cold crystallization peak appears at 101°C. This trend is observed for C_0 = 0.09 – 5.0wt%, T_c varying from 78 to 81°C. In the range 140 – 180°C, multiple exothermic process is observed in the nonreversing heat flow trace suggesting complicated melting process: this probably contains the transition from the less ordered α' phase to the ordered α phase, and/or melting-recrystallization-remelting process [14,15]. In the glass transition temperature range, an intense endotherm in the nonreversing heat flow trace is observed, which is attributed to the enthalpy overshoot due to physical aging. This is due to the long time aging in the vacuum drying process at 40°C for 168 h.

We should note here that the FDPLLA with C_0 = 5.0wt% exhibits T_c depression. The critical concentration of chain overlapping has been estimated to be 0.3wt% for the present PLLA (M_w = 210 kg mol^{-1}) [9], thus the assumption of less chain overlapping for FDPLLA cannot explain the present T_c depression. We should also note that in contrast to T_c, the present solvent-free FDPLLA exhibits no T_g shift from the bulk value as shown in Fig. 2 (58 – 60°C). This may be reasonably understood by considering the difference in sensitivity to the free surface between the T_c and T_g as will be discussed later.

Figure 3 shows the overall crystallization rate of isothermal cold crystallization with respect to crystallization temperature. The FDPLLAs exhibit higher crystallization rate than the bulk PLLA in the whole temperature range investigated. In addition, the temperature for the maximum G value (90 – 110°C) is lower for the FDPLLAs than for

the bulk (ca. 120°C), and this tendency is prominent for lower C_0. It is also noted that FDPLLAs with C_0 = 0.50 and 0.09wt% exhibit only a little difference in the profile; this point will be discussed later. It has been reported that the growth rate of PLLA from the melt exhibits a discontinuous profile at 113°C [16]. However, the profiles in Fig. 3 for FDPLLA with C_0 = 5.0wt% and the bulk show no apparent discontinuous change. This might be due to the thermal process of the present experiments which is different from that of the melt crystallization. Since the temperature jumps were not instantaneous, structural change may commence before reaching the predetermined crystallization temperature, and the early stage of crystallization may be governed by the mechanism of the lower temperature regime even for higher predetermined crystallization temperatures.

The higher crystallization rates for FDPLLAs are consistent with the T_c depression. Furthermore, we found that the degree of crystallinity achieved after isothermal cold crystallization for 30 min is higher for the FDPLLAs (0.05 – 0.21) than for the bulk (0.02 – 0.08) in the temperature range investigated. It is pertinent to assume that the high crystallizability of FDPLLAs is originated from higher mobility of the polymer chain which is specific to the freeze-dried state with high surface-to-volume ratio as will be discussed in the next section. Based on this assumption, we analyze the results in Fig. 3. To this end, we here assume that the overall crystallization rate is mainly governed by the surface nucleation process [17,18] (this assumption is adopted just for a rough estimation of relative mobility; actually it is uncertain whether primary nucleation process has little contribution to overall crystallization). In this case, G is given by

$$G = G_0 \exp\left[-\frac{U}{R(T-T_0)}\right]\exp\left[-\frac{K_g}{T\Delta T}\right] \qquad (1)$$

where G_0 is a prefactor, U the activation energy for the chain diffusion process, R the gas constant, T_0 the Vogel temperature, ΔT the supercooling ($T_m^\circ - T$), and K_g a constant that depends on the three regimes. Based on the present assumption, the equilibrium melting temperature T_m° and surface free energies of the nucleus for the FDPLLA are the same as those for the bulk PLLA. This means that the observed difference between G vs T profiles for the freeze-dried and bulk PLLAs is attributed to the difference in the diffusion aspect. Using Eq (1), we executed fitting analysis: we first determined the parameter K_g to be 3.0×10^5 K^2, which is common to all of the curves, so as to give

linear relationship between ln $G + K_g/(T\Delta T)$ and $1/(T - T_0)$ for all the profiles. Then, we determined the best fit value of U for each profile by linear regression method as shown in Fig. 4. Here, we used literature values $T_m^\circ = 478$ K [19] and $T_0 = T_g - 30$ K [20]. As for $C_0 = 0.50$ and 0.09wt%, the fitting analysis was done in a limited temperature range below 110°C where crystallization rate is apparently greater than that for $C_0 = 5.0$wt%. The obtained values of U for FDPLLAs are 4.0 kJ mol^{-1} for $C_0 =$ 0.50 and 0.09wt%, and 4.3 kJ mol^{-1} for $C_0 = 5.0$wt%, while that of the bulk is 6.4 kJ mol^{-1}, indicating lower energy barriers for elementary motions in FDPLLA that concern cold crystallization than in the bulk. Incidentally, the bulk value for U obtained above is in good agreement with the literature value obtained for spherulitic growth rate from the melt [20].

Free surface effect

Two possible origins for the higher crystallizability of FDPLLA demonstrated above may be considered, i.e., the surface effect and the configuration effect. As the FDPLLA is very porous with large free surface area, the surface effect is considered to become prominent. Near the free surface, the chain segments have higher mobility, thus are subject to lower barrier U for the diffusion across the crystalline-amorphous interface. Figure 5 shows SEM images for the present FDPLLA. Inside the sphere-shaped particle is very porous consisting of a lot of thin membranes that form fine tissue. The surface of the particle is also porous as shown in Fig. 5 (c). The porous architecture of the FDPLLA has probably formed during the sublimation process.

The specific surface area evaluated from the observed BET isotherms is presented in Table 1 together with T_c values. The thickness of a flat film that has the same specific surface area (d_f) is also shown. For this estimation, we used a value 1.248 g cm^{-3} for the density of completely amorphous PLLA [21]. Thus, the average thickness of the membrane composing the porous architecture of the present FDPLLA is estimated to be at most 104 – 135 nm. We see that the dependence of the specific surface area on C_0 is rather weak. This suggests that segregation of PLLA from the solvent (phase separation) occurs rapidly during the freezing process so that the effect of C_0 on the resulting structure with fine membranes is limited. The rapid segregation during

freezing is supported by the estimated diffusion coefficient of PLLA as discussed in the previous paper [9]. On the other hand, we found from the sink-float method that the density of the FDPLLA is identical to the bulk amorphous density within the experimental error.

The high porosity with no density difference from the bulk value suggests that the free surface effect plays a dominant role in the specific cold crystallization behavior of FDPLLA. This is evidenced by the results in Fig. 3 that cold crystallization is enhanced as C_0 decreases, i.e., as the specific surface area increases (Table 1). However, the difference in crystallization rate between FDPLLAs with C_0 = 0.50 and 0.09wt% is rather small, and furthermore, for higher crystallization temperatures (> 110°C), the C_0 dependence seems to be very little in the range of C_0 = 0.09 – 5.0wt%. This may be due to instability of the structure with high porosity in the FDPLLA. At higher temperatures well above T_g, the unstable porous structure may collapse due to structural relaxation to some extent before the crystallization commences. Also, the instability of the structure may be higher for lower C_0, thus, for the sample from 0.09wt% solution, the porous structure easily undergoes collapse to the structure of higher C_0 even at low temperatures below 110°C.

To check further the free surface effect mentioned above, we performed DSC step-scan measurements for samples immersed in ligroin (non-solvent for PLLA). The observed T_c and T_g values are listed in Table 2. The magnitude of T_c depression becomes larger for the FDPLLA/ligroin mixture, while the bulk PLLA undergoes little T_c depression. Most likely this additional T_c depression for the FDPLLA is due to different interaction at the interface (PLLA/ligroin and PLLA/air), i.e., the feature of interface significantly affects the cold crystallization behavior. The result strongly supports the idea that the high crystallizability of FDPLLA is mainly due to its large surface area. One might speculate that swelling at the PLLA/ligroin interface occurs, resulting in the enhancement of mobility. We observed no macroscopic swelling at all even after immersion for 30 days at room temperature. Nevertheless, there might be a swollen region near the interface on molecular scale, which is responsible for the enhanced mobility. Table 2 shows that T_g is also lowered for the FDPLLA/ligroin mixture. This might suggest the above microscopic swelling at the interface.

Here we should note again that T_c is significantly reduced by freeze-drying whereas

T_g is not affected as shown in Fig. 2. The above estimated membrane thickness 135 nm is not low enough to occur the size effect on T_g for polymer thin films: in general, the effect appears for thicknesses below 100 nm [22]. Thus, no change in T_g for the present result seems to be reasonable. On the other hand, there is considerable evidence that the polymer dynamics near a free surface is different from that in the bulk state [22-26]. Assuming higher mobility near the surface than in the bulk, the cold crystallization may be promoted exclusively in the surface region. If the crystallization occurs much slower in the inner bulk-like part of the membrane than in the surface region, the cold crystallization signal detected by calorimetry is responsible exclusively for the fast crystallization events from the surface region. In contrast, the glass transition reflects the contributions from the whole part of the membrane containing the inner part. In this sense, the cold crystallization is more 'surface-sensitive' than the glass transition event.

Structural characterization

It has been argued whether the specific structure exists in freeze-dried polymer materials [2-11]. For the depression of T_g for freeze-dried polymers, the residual solvent has been demonstrated to be a dominant cause in spite of various other explanations [12]. On the other hand, there seems to be no direct evidence for less entangled configuration in freeze-dried polymers, while chain interpenetration as in the bulk state has been demonstrated to occur [11]. Figure 6 shows comparison of the WAXS profiles of FDPLLA (C_0 = 0.50wt%) and the bulk PLLA. No diffraction peak from crystalline structure is observed, which indicates that both the freeze-dried and bulk PLLAs are completely amorphous. The profiles closely coincide with each other within the experimental error. This indicates that the amorphous structure of the mobile surface layer is very similar to that of the bulk structure, or its contribution is too small to be detected by the present WAXS analysis. In spite of such little difference in WAXS profiles, the crystallization rate is largely enhanced in the FDPLLA. This again suggests the surface-sensitivity of the crystallization event as we discussed in the preceding subsection.

As another possible structural origin for the enhanced cold crystallization, one could assume that the chain conformation in FDPLLA is different from that in the bulk PLLA,

i.e., the freeze-drying might raise the population of crystalline-like conformations such as the left-handed –10/3 helix [27]. However, we found no significant difference in FT-IR spectrum between the freeze-dried and bulk PLLAs as shown in Fig. 7 (a): we found no apparent absorption band at 921 cm^{-1} (assigned to the helical conformation [28]) for both the samples. Also, characteristic shift of the band at ca. 870 cm^{-1} to a higher wavenumber (assigned to intermolecular packing [28,29]) did not occur for both the samples. Recently, it has been shown that in the cold crystallization process of PLLA, the helix conformation is formed first, which is followed by crystalline perfection [30]. Based on this finding, it can be said that the structure of the present FDPLLAs is not even on the road to crystallization from a view point of the local chain conformation.

Other possible origins

It has been reported for PLLA that crystalline nucleation occurs during rapid cooling from the melt to the glassy state even if crystallization does not occur, and that the rate of subsequent cold crystallization depends on the number of crystal nuclei, which can be controlled by the quenching rate [31]. We investigated the cold crystallization temperature T_c for the present bulk PLLA which had been quenched from the melt at different cooling rates of 5 – 100 K min^{-1}, but no significant dependence on the quenching rate was observed. It is considered from this result that if for some reason, the nucleus density was higher for as-freeze-dried PLLA than for the bulk, this would not cause the observed T_c depression of as large as 20 K.

Next, we discuss the effect of the rigid amorphous phase where the segmental mobility is lower than in a usual amorphous phase. Such rigid amorphous has been demonstrated to occur for various semi-crystalline polymers including PLLA [9,32-34]. One might consider that the T_c depression is due to the absence of rigid amorphous in the FDPLLA, that is, the bulk PLLA quenched from the melt would still contain some rigid amorphous portion of which the T_g might be even higher than the crystal melting range, while the FDPLLA contains no rigid amorphous because it has undergone the solution state. Figure 7 (b) shows the reversing heat capacity traces around T_g for the freeze-dried and amorphous bulk PLLAs. We see that the heat capacity jump at T_g for the FDPLLA is approximately the same as that for the bulk (ΔC_p = ca. 0.5 J g^{-1} K^{-1}).

In addition, the absolute values of heat capacity at 70°C (just above T_g) for these samples coincide with the reported value for the liquid state of PLLA [35]. These findings indicate that the amorphous fraction which undergoes glass transition at around 60°C in the FDPLLA is the same as that for the bulk, and that no rigid amorphous exists in both the freeze-dried and bulk PLLAs. We thus conclude that the absence of the rigid amorphous is not the cause of the T_c depression. Incidentally, the decrease in heat capacity just above T_g for the FDPLLA is due to cold crystallization [9].

It has been claimed that the physical aging enhances the rate of crystallization [29,36,37]. In the present PLLA samples, both the freeze-dried and bulk PLLAs have been subjected to the same annealing process at 40°C for 168 h under vacuum, thus, the physical aging effect is not responsible for the observed difference concerning the cold crystallization behaviors. Furthermore, we found that an FDPLLA without the annealing process exhibits the same magnitude of T_c depression, and that it gives an identical WAXS profile to that of the annealed FDPLLA.

CONCLUSIONS

We have confirmed that the present FDPLLAs exhibit lowered T_c as well as enhanced cold crystallization rates compared with the bulk PLLA. We observed no major difference in the local amorphous structure, chain conformations, and density from those of the bulk PLLA, and we conclude that the origin of the higher crystallizability of FDPLLAs is due to its high surface-to-volume ratio rather than some specific structure created by the freeze-drying process. It is reasonable to assume that the chain mobility is enhanced at the polymer/air interface, where the cold crystallization rate is considerably raised. Further depression of T_c was observed for the FDPLLA immersed in ligroin, which supports the above conclusion. No apparent difference in WAXS profile was observed between the freeze-dried and bulk PLLAs, suggesting very small difference in the amorphous structure or very small contribution, of the mobile surface region.

ACKNOWLEDGEMENT

This work was supported by a Grant-in-Aid for Scientific Research (No. 18550107) from the Ministry of Education, Culture, Sports, Science, and Technology of Japan.

The authors thank Saori Morita for help in preparing the freeze-dried samples. Prof. Koji Nakane is also acknowledged for the measurements of specific surface area.

REFERENCES

1. P. L. Chang and H. Morawetz, *Macromolecules*, **20**, 428 (1987).
2. J. Ding, G. Xue, Q. Dai, and R. Cheng, *Polymer*, **34**, 3325 (1993).
3. G. Xue, Y. Lu, G. Shi, and Q. Dai, *Polymer*, **35**, 892 (1994).
4. G. Ji, G. Xue, J. Ma, C. Dong, and X. Gu, *Polymer*, **37**, 3255 (1996).
5. T. Sasaki, M. Tanaka, and T. Takahashi, *Polymer*, **39**, 3853 (1998).
6. Y. Li and G. Xue, *Polymer*, **40**, 3165 (1999).
7. P. Bernazzani, S. L. Simon, D. J. Plazek, and K. L. Ngai, *Eur. Phys. J. E*, **8**, 201 (2002).
8. S. L. Simon, P. Bernazzani, and G. B. McKenna, *Polymer*, 44, 8025 (2003).
9. T. Sasaki, N. Yamauchi, S. Irie, and K. Sakurai, *J. Polym. Sci. Part B: Polym. Phys.*, **43**, 115 (2005).
10. K. J. McGrath and C. M. Roland, *Macromolecules*, **25**, 1366 (1992).
11. K. J. McGrath, C. M. Roland, and R. G. Weiss, *Macromolecules*, **26**, 6127 (1993).
12. W. Zheng and S. L. Simon, *Polymer*, **47**, 3520 (2006).
13. R. C. Allen and L. Mandelkern *Polym. Bull.*, **17**, 473 (1987).
14. T. Kawai, N. Rahman, G. Matsuba, K. Nishida, T. Kanaya, M. Nakano, H. Okamoto, J. Kawada, A. Usuki, N. Honma, K. Nakajima, and M. Matsuda, *Macromolecules*, **40**, 9463 (2007).
15. M. Yasuniwa, K. Iura, and Y. Dan, *Polymer*, **48**, 5398 (2007).
16. M. Yasuniwa, S. Tsubakihara, K. Iura, Y. Ono, Y. Dan, and K. Takahashi, *Polymer*, **47**, 7554 (2006).
17. K. Armitstead and G. Goldbeck-Wood, *Adv. Polym. Sci.*, **100**, 219 (1992).
18. J. D. Hoffman and R. L. Miller, *Polymer*, **38**, 3151 (1997).
19. H. Tsuji and Y. Ikada, *Polymer*, **36**, 2709 (1995).
20. R. Vasanthakumari and A. J. Pennings, *Polymer*, **24**, 175 (1983).
21. E. W. Fischer, H. J. Sterzel, and G. Wegner, *Kolloid Z. Z. Polymere*, **251**, 980 (1973).
22. J. A. Forrest and K. Dalnoki-Veress, *Adv. Colloid Interface Sci.*, **94**, 167 (2001).
23. JL Keddie, R. A. L. Jones, and RA Cory, *Europhys. Lett.*, **27**, 59 (1994).

24. K. Fukao and Y. Miyamoto, *Phys. Rev. E*, **61**, 1743 (2000).
25. K. Akabori, K. Tanaka, T. Kajiyama, and A. Takahara, *Macromolecules*, **36**, 4937 (2003).
26. T. Sasaki, A. Shimizu, T. H. Mourey, C. T. Thurau, and M. D. Ediger, *J. Chem. Phys.*, **119**, 8730 (2003).
27. W. Hoogsteen, A. R. Postema, A. J. Pennings, G. ten Brinke, and P. Zugenmaier, *Macromolecules*, **23**, 634 (1990).
28. J. Zhang, H. Tsuji, I. Noda, and Y. Ozaki, *J. Phy.s Chem. B*, **108**, 11514 (2004).
29. P. Pan, Z. Liang, B. Zhu, T. Dong, and Y. Inoue, *Macromolecules*, **41**, 8011 (2008).
30. B. Na, N. Tian, R. Lv, Z. Li, W. Xu, and Q. Fu *Polymer*, **51**, 563 (2010).
31. M. Salmerón Sánchez, V. B. F. Mathot, G. V. Poel, and J. L. Gómez Ribelles, *Macromolecules*, **40**, 7989 (2007).
32. B. Wunderlich, *Progr. Colloid Polym. Sci.*, **96**, 22 (1994).
33. I. Okazaki and B. Wunderlich, *J. Polym. Sci. Part B: Polym. Phys.*, **34**, 2941 (1996).
34. M. Arnoult, E. Dargent, and J. F. Mano, *Polymer*, **48**, 1012 (2007).
35. M. Pyda, R. C. Bopp, and B. Wunderlich, *J. Chem. Thermodyn.*, **36**, 731 (2004).
36. P. Pan, B. Zhu, and Y. Inoue, *Macromolecules*, **40**, 9664 (2007).
37. P. Pan, B. Zhu, T. Dong, K. Yazawa, T. Shimizu, M. Tansho, and Y. Inoue, *J. Chem. Phys.*, **129**, 184902 (2008).

FIG. 1. Freeze-dried PLLA particles prepared from 5.0wt% 1,4-dioxane solution. The inner part of the particle is very porous as shown in Fig. 5.

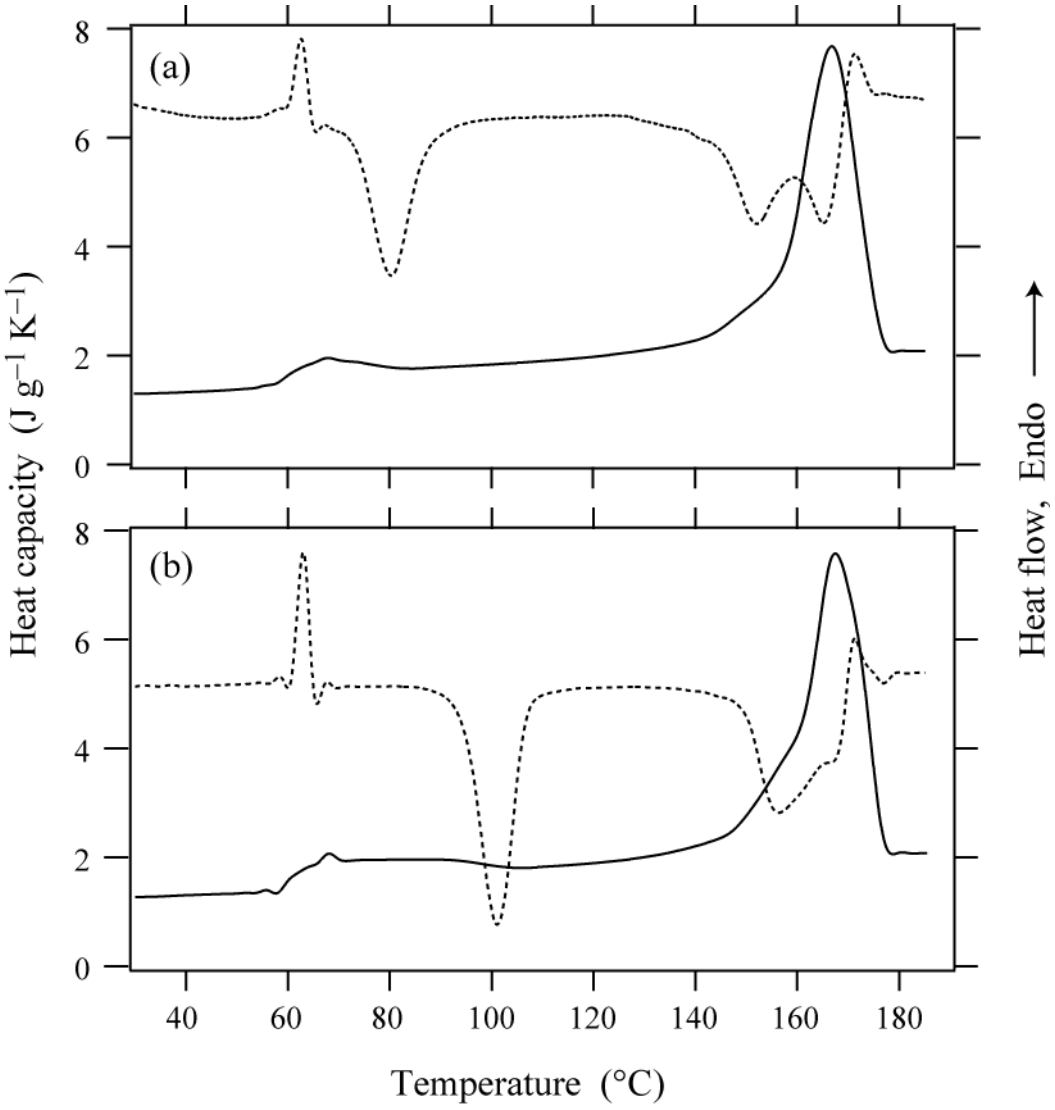

FIG. 2. DSC traces obtained from the step-scan measurements for (a) FDPLLA of C_0 = 5.0wt%, and (b) bulk PLLA. The solid curves indicate reversing heat capacity and the dotted curves indicate nonreversing heat flow (arbitrary units).

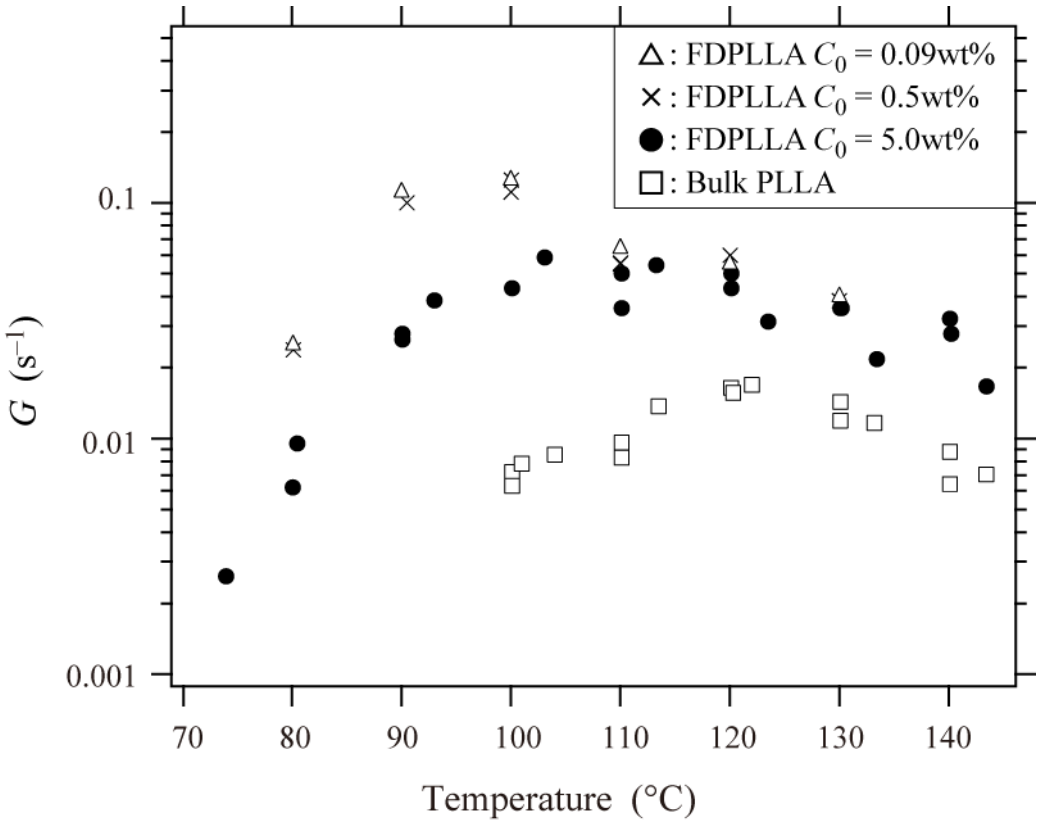

FIG. 3. Isothermal cold crystallization rate G (= $1/t_{0.5}$) plotted against crystallization temperature.

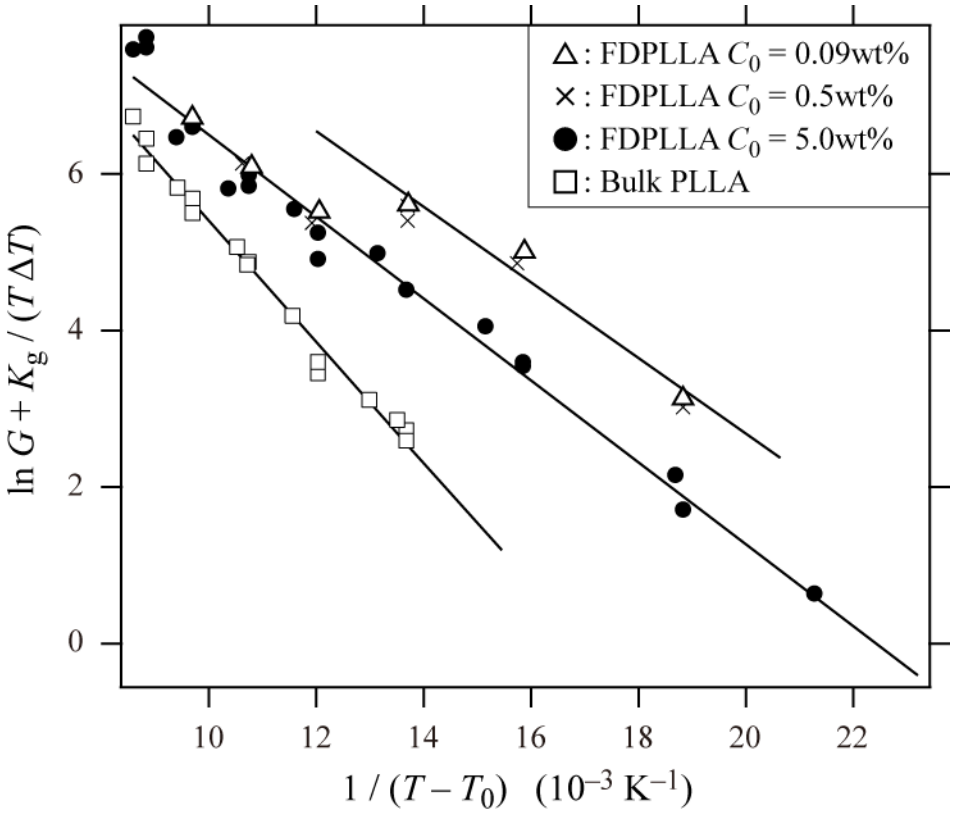

FIG. 4. Plots of ln $G + K_g/(T\Delta T)$ vs $1/(T - T_0)$ for the FDPLLAs and bulk PLLA. The solid lines are the results of linear regression analysis based on the surface nucleation theory. As the profiles for FDPLLA of C_0 = 0.50 and 0.09wt% are very similar to each other, only one linear regression line is presented (C_0 = 0.50wt%).

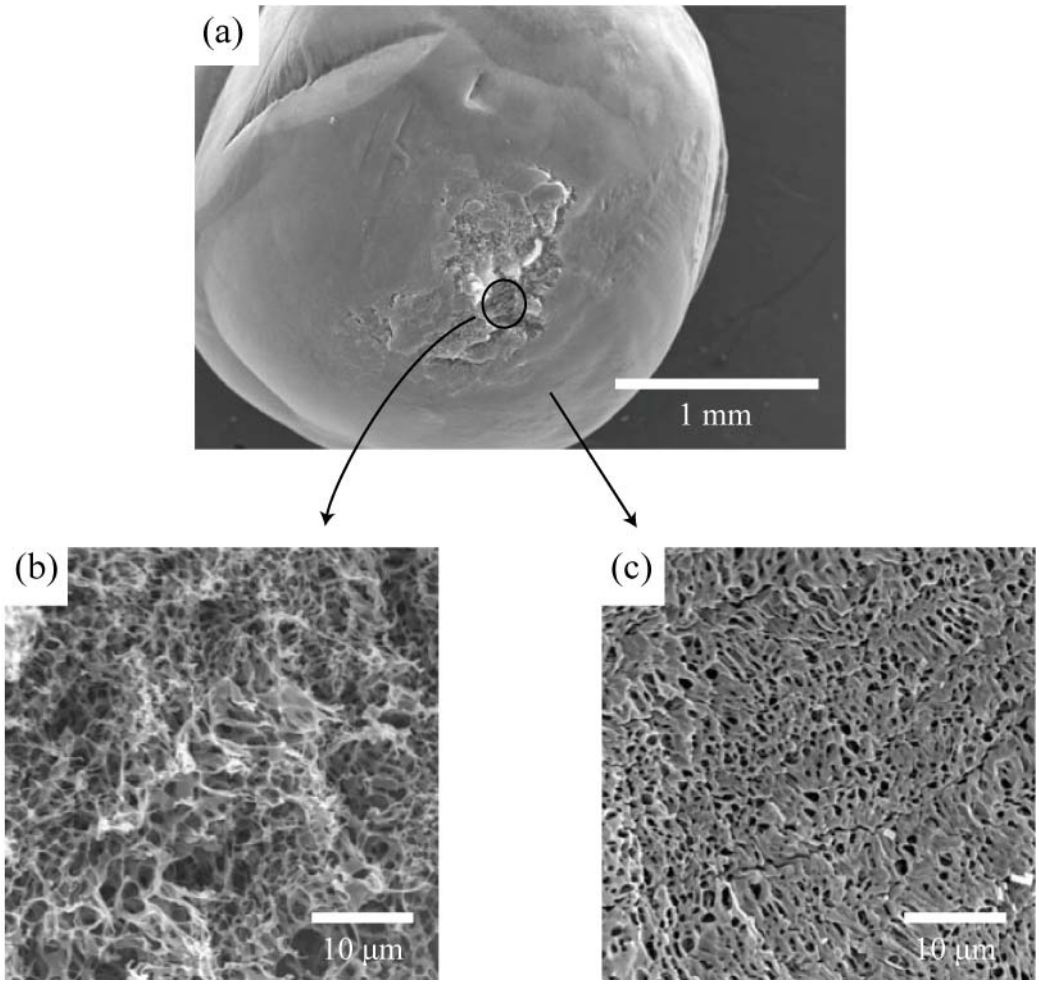

FIG. 5. SEM images of FDPLLA particle (C_0 = 5.0wt%). A small part of the surface indicated by the circle in (a) was peeled off with adhesive tape to observe the inside of the particle. Expanded images for the inner part and the surface are shown in (b) and (c), respectively.

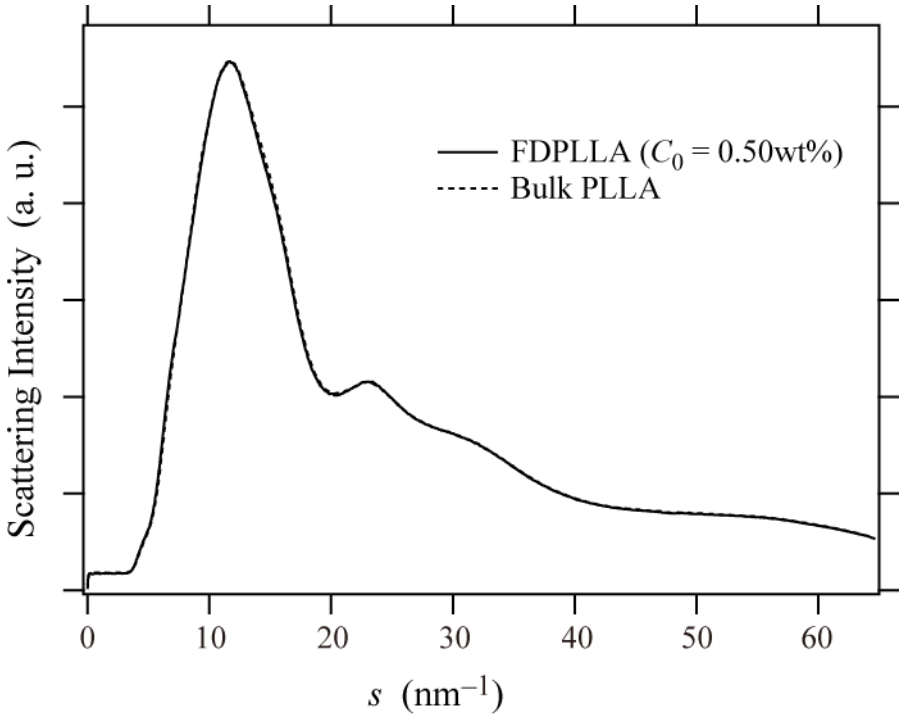

FIG. 6. WAXS profiles for the FDPLLA (C_0 = 0.50wt%) and bulk PLLA ($s = 4\pi \sin\theta / \lambda$). No distinct difference is observed between the two profiles.

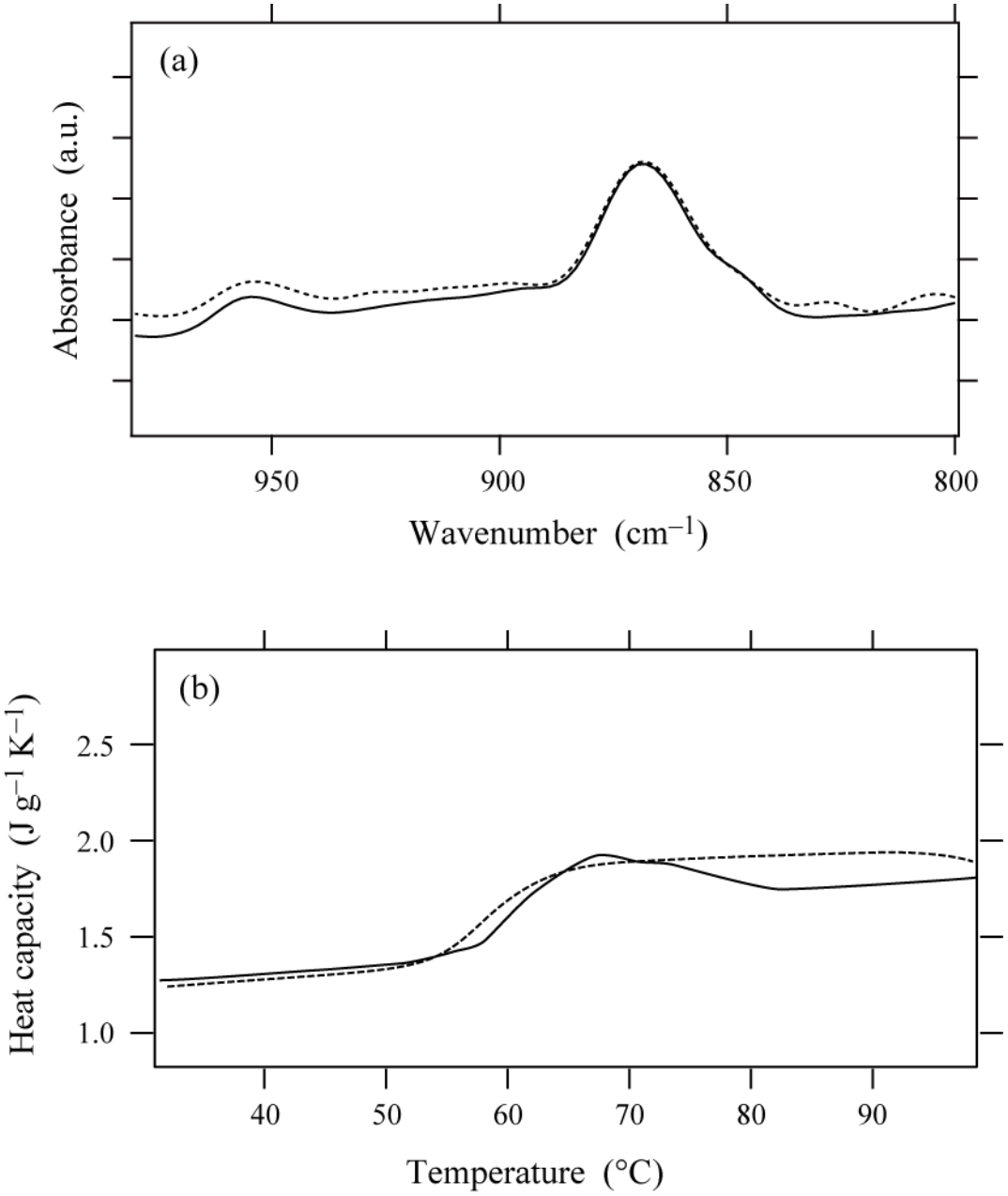

FIG. 7. FT-IR spectra (a) and reversing heat capacity around the glass transition temperature (b), for as-freeze-dried PLLA of C_0 = 5.0wt% (solid curve) and quenched bulk PLLA (dotted curve).